JPn Neuroscience

The Journal of Physiology

J Physiol 590.10 (2012) pp 2409–2425

Are all spinal segments equal: intrinsic membrane properties of superficial dorsal horn neurons in the developing and mature mouse spinal cord

M. A. Tadros, B. M. Harris, W. B. Anderson, A. M. Brichta, B. A. Graham and R. J. Callister

School of Biomedical Sciences and Pharmacy, Faculty of Health and Hunter Medical Research Institute, University of Newcastle, Callaghan, NSW 2308, Australia

Key points

- Much of what we know about pain signalling in the spinal cord comes from studies undertaken in lumbosacral spinal segments that innervate the hindlimb.
- Clinical evidence suggests sensory information from viscera and head and neck tissues is processed differently from sensations arising in the hindlimb.
- Here we show that intrinsic membrane properties, a major determinate of neuronal output, change dramatically during development in superficial dorsal horn (SDH) neurons from lumbar, thoracic and upper cervical segments in the mouse. In contrast, intrinsic membrane properties are generally conserved in SDH neurons along the length of the spinal cord in both neonates and adults.
- Our data suggest the intrinsic membrane properties of SDH neurons involved in pain signalling do not contribute to the marked differences in pain experienced in the limbs, viscera and head and neck.

Abstract Neurons in the superficial dorsal horn (SDH; laminae I–II) of the spinal cord process nociceptive information from skin, muscle, joints and viscera. Most of what we know about the intrinsic properties of SDH neurons comes from studies in lumbar segments of the cord even though clinical evidence suggests nociceptive signals from viscera and head and neck tissues are processed differently. This 'lumbar-centric' view of spinal pain processing mechanisms also applies to developing SDH neurons. Here we ask whether the intrinsic membrane properties of SDH neurons differ across spinal cord segments in both the developing and mature spinal cord. Whole cell recordings were made from SDH neurons in slices of upper cervical (C2–4), thoracic (T8–10) and lumbar (L3–5) segments in neonatal (P0–5) and adult (P24–45) mice. Neuronal input resistance (R_{IN}), resting membrane potential, AP amplitude, half-width and AHP amplitude were similar across spinal cord regions in both neonates and adults (~100 neurons for each region and age). In contrast, these intrinsic membrane properties differed dramatically *between* neonates and adults. Five types of AP discharge were observed during depolarizing current injection. In neonates, single spiking dominated (~40%) and the proportions of each discharge category did not differ across spinal regions. In adults, initial bursting dominated in each spinal region, but was significantly more prevalent in rostral segments (49% of neurons in C2–4 *vs.* 29% in L3–5). During development the dominant AP discharge pattern changed from single spiking to initial bursting. The rapid A-type potassium current (I_{Ar}) dominated in neonates and adults, but its prevalence decreased (~80% *vs.* ~50% of neurons) in all regions during development. I_{Ar} steady state inactivation and activation also changed in upper cervical and lumbar regions during

DOI: 10.1113/jphysiol.2012.227389

development. Together, our data show the intrinsic properties of SDH neurons are generally conserved in the three spinal cord regions examined in both neonate and adult mice. We propose the conserved intrinsic membrane properties of SDH neurons along the length of the spinal cord cannot explain the marked differences in pain experienced in the limbs, viscera, and head and neck.

(Resubmitted 1 January 2012; accepted after revision 15 February 2012; first published online 20 February 2012)
Corresponding author R. J. Callister: School of Biomedical Sciences and Pharmacy, University of Newcastle, Callaghan, NSW 2308, Australia. Email: robert.callister@newcastle.edu.au

Abbreviations AP, action potential; I_{Ar}, rapid A-type potassium current; I_{As}, slow A-type potassium current; RMP, resting membrane potential; SDH, superficial dorsal horn.

Introduction

The superficial dorsal horn (SDH; laminae I–II) of the spinal cord is the first central processing site in the ascending pain pathway. The mechanisms by which signals from skin, muscle, joints and viscera are processed in the SDH have been investigated extensively in order to understand central pain mechanisms (Zeilhofer, 2005; Graham *et al.* 2007*a*; Willis Jr, 2007). Most studies focus on the lumbar spinal cord because it is readily accessed for *in vivo* electrophysiology (Graham *et al.* 2004; Andrew, 2009), and provides slices with long dorsal roots for electrical stimulation (Yoshimura & Jessell, 1989*b*; Ikeda *et al.* 2006). Additionally, the lumbar cord permits concomitant behavioural and electrophysiological investigations of spinal pain processing mechanisms in preparations that involve damaging peripheral nerves or inflaming the skin of the hindpaw (Berberich *et al.* 1988; Daniele & MacDermott, 2009).

In spite of the focus on the lumbar region of the cord it is important to note that other spinal segments/regions receive signals from very different combinations of tissues and, based on animal work and clinical presentation, there is evidence that nociceptive processing mechanisms differ between spinal regions. For example, upper cervical (C1–C4) superficial dorsal horn neurons receive convergent input from widely differing structures in the head and neck including skin, muscle, joints and intracranial blood vessels (Kaube *et al.* 1993; Strassman *et al.* 1994; Zhou *et al.* 1999; Hu *et al.* 2005; Panfil *et al.* 2006; Morch *et al.* 2007; Liu *et al.* 2008). Moreover, patients presenting with pain originating in these structures often complain of a long list of ailments, including impaired postural control and sense of balance, visual disturbances, general weakness, numbness or parathesis, cutaneous hyperalgesia, and psychological symptoms such as disturbances in concentration and memory (Barnsley *et al.* 1994; Vuillerme & Pinsault, 2009). These presenting signs and symptoms are not normally associated with chronic pain originating in the limbs where pain and sensory disturbances tend to be more specific (Sterling *et al.* 2003).

Like upper cervical segments, the thoracic region of the cord also differs markedly from the lumbar region as it receives significant input from organs in the thorax, abdomen and pelvis (Kuo *et al.* 1983; Kuo & de Groat, 1985; Qin *et al.* 2007). Anatomical studies in cat have shown convergence of visceral and cutaneous primary afferent inputs in the dorsal horn of the thoracic spinal cord (Cervero & Connell, 1984). This convergence has also been confirmed electrophysiologically, with approximately two-thirds of SDH neurons in T8–T12 spinal segments responding to both somatic and visceral primary afferent stimulation (Cervero & Tattersall, 1987). Similarly, convergent inputs from cutaneous and visceral structures are also widespread in the mouse spinal cord (Jobling *et al.* 2010). Clinically, pain emanating from visceral structures in the thorax, abdomen and pelvis presents differently to limb pain and is characterized by referral to somatic sites including skin and muscle, referral to other viscera (i.e. viscero-visceral hyperalgesia), and poorly defined localization (Cervero & Laird, 1999; Giamberardino, 1999).

There are also differences in the development of spinal cord segments from cervical to sacral regions. During embryonic development, the neural tube closes at the hindbrain/cervical boundary, and then seals caudally to form the spinal cord (O'Rahilly & Muller, 2002; Copp *et al.* 2003). Reflex responses then develop along a rostrocaudal gradient, with reflex movements to head and forelimb stimulation occurring at E16 and hindlimb stimulation later at E18 in the rat (Narayanan *et al.* 1971). Human embryos also exhibit head and neck movement before they move their limbs (Humphrey, 1969). Interestingly, the overwhelming majority of studies on the development of spinal pain mechanisms have also focused on lumbosacral regions for the same reasons outlined above for adults.

Regardless of spinal cord region or developmental stage, the output of SDH neurons in spinal circuits is determined by the combined action of their intrinsic membrane properties and synaptic connections (Turrigiano *et al.* 1994; Willis & Coggeshall, 2004). Here we ask whether the intrinsic membrane properties of SDH neurons differ in three distinct spinal cord regions that receive widely

differing peripheral input and levels of convergence from various tissue types in both neonatal and adult mice.

Methods

Preparation of spinal cord slices

The University of Newcastle Animal Care and Ethics Committee approved all procedures used in this study and they comply with the policies and regulations of *The Journal of Physiology* as outlined by Drummond (2009). Mice (C57Bl/6, both sexes) were divided into two age groups, P0–5 (hereafter termed neonates) and P24–45 (adults). These ages were selected as they represent developmental stages either side of a critical period in the development of electrophysiological properties in lumbar SDH neurons (Walsh *et al.* 2009). Approximately equal numbers of male and female mice were used in our experiments (46% *vs.* 54%, respectively).

Neonatal mice were immersed in ice to induce hypothermia and adult animals were anaesthetized with ketamine (100 mg kg^{-1} I.P.). Once deep hypothermia or anaesthesia was achieved, animals were decapitated and the vertebral column and posterior thoracic wall were rapidly isolated and immersed in ice-cold oxygenated sucrose substituted artificial cerebrospinal fluid (S-ACSF) containing (in mM): 250 sucrose, 25 $NaHCO_2$, 10 glucose, 2.5 KCl, 1 NaH_2PO_4, 1 $MgCl_2$ and 2.5 $CaCl_2$. The S-ACSF was continually bubbled with 95% O_2–5% CO_2 to maintain a pH of 7.3–7.4. Lengths of vertebral column containing upper cervical (C2–4), thoracic (T8–10) or lumbar (L3–5) spinal cord segments were isolated and the corresponding spinal cord region was removed. Transverse slices were prepared using previously described techniques (Graham *et al.* 2008). The isolated spinal cord region was placed on a Styrofoam support-block. The block and spinal cord were then glued to a cutting stage with cyanoacrylate glue (Loctite 454, Loctite, Caringbah, Australia) and transverse slices (400 μm thick for neonates; 300 μm for adults) were obtained using a vibrating blade microtome (Microm HM650, Microm International GmbH, Germany). Slices were transferred to an interface storage chamber containing oxygenated ACSF (118 mM NaCl substituted for sucrose in S-ACSF) and allowed to recover for 1 h at room temperature (22–24°C) before recording commenced.

Electrophysiology

Slices were transferred to a recording chamber (volume 0.4 ml) and continually superfused (4–6 chamber volumes/min) with ACSF. Recording temperature was maintained at near-physiological temperature (32°C) using an in-line temperature control unit (Model TC324B, Warner Instruments, Hamden, CT, USA). Whole cell patch clamp recordings were obtained from SDH neurons using an Axopatch 200B amplifier (Molecular Devices, Sunnyvale, CA, USA). Individual neurons were visualized using infrared differential interference contrast optics and an infrared-sensitive camera (Hamamastu C2400-79C, Hamamatsu City, Japan). In adult mice, the substantia gelatinosa (lamina II) appears as a translucent band and recordings were made from neurons located within or dorsal to this region. In neonatal mice this translucent band is not apparent, due to the lack of myelination at this age, so recordings in neonates were restricted to within 140 μm of dorsal surface of the slice as this corresponds to the limit of lamina II in Nissl stained slices of P2 animals (Walsh *et al.* 2009).

Patch pipettes (2–5 MΩ resistance) were filled with a potassium methylsulphate-based internal solution containing (in mM): 135 KCH_3SO_4, 6 NaCl, 2 $MgCl_2$, 10 Hepes, 0.1 EGTA, 2 MgATP and 0.3 NaGTP (pH adjusted to 7.3 with KOH). The whole cell recording mode was first established in voltage clamp (holding potential −60 mV, series resistance <20 MΩ). Input resistance (R_{IN}) was measured from the averaged response (5 trials) to a 5 mV hyperpolarizing step. This value was examined at the beginning and end of each recording session and data were rejected if it changed by >20%. We next tested for the presence of the four major subthreshold currents known to exist in rodent SDH neurons (Yoshimura & Jessell, 1989*a*; Ruscheweyh & Sandkuhler, 2002; Graham *et al.* 2007*c*). This was achieved by delivering a hyperpolarizing pulse (to −90 mV, 1 s duration), followed by a depolarizing step (to −40 mV, 200 ms duration). The protocol was repeated five times to obtain an average for analysis. This protocol identified the four major subthreshold currents described previously, including the outward potassium currents rapid A (I_{Ar}) and slow A (I_{As}), the inward T-type calcium current (I_{Ca}), and the non-specific cationic H current (I_H). In a recent study, we have confirmed the identity of these currents in mouse SDH neurons according to their sensitivity to 4AP, nickel and caesium, respectively (see Graham *et al.* 2007*c*). We restricted the depolarizing step to −40 mV to avoid activation of tetrodotoxin-sensitive Na^+ and delayed rectifier channels (Safronov, 1999). Capacitive and leakage currents were removed via the automated P/N leak subtraction method within the Axograph software.

For neurons displaying I_{Ar}, voltage-dependent activation and steady state inactivation were further assessed using two protocols. Voltage-dependent activation was measured by applying a hyperpolarizing pulse to −90 mV (1 s duration), followed by a series of depolarizing voltage steps of increasing amplitude (from −85 mV to −40 mV, 5 mV increments, 200 ms duration). I_{Ar} steady state inactivation was assessed by application of a series of hyperpolarizing prepulses (from −90 mV to

−40 mV, 5 mV increments, 1 s duration), followed by a depolarizing voltage step to −40 mV (200 ms duration).

After running the above protocols, the recording mode was switched to current clamp. The membrane potential observed ∼15 s after this switch was considered to be resting membrane potential (RMP) and all current clamp recordings were made from this potential. All reported membrane potentials were corrected for a 10 mV junction potential (Barry & Lynch, 1991). Individual action potential (AP) properties and discharge characteristics were examined by injecting a series of depolarizing and hyperpolarizing current steps (800 ms duration, 20 pA increments, delivered every 8 s).

At the end of each recording session, the location of the recorded neuron was mapped as described previously (Graham *et al.* 2007*c*). Briefly, digital images of the spinal cord slice with the electrode still attached to the neuron were captured using a Rolera-XR digital camera, and QCapture Pro software (Spectra Services, Rochester, NY, USA). The image was then imported into Adobe Illustrator and manipulated so the dorsal horns aligned. A standardized template of the relevant spinal cord segment was then resized until it could be overlaid on the dorsal grey matter borders of the imported image. The location of the recorded neuron was plotted on these standardized templates. For neonates, templates were from the spinal cord of a P4 mouse (courtesy of Charles Watson and Gulgun Kayalioglu). Adult templates were from Watson *et al.* (2009).

Data capture and analysis

Data were digitized online (sampled at 10 kHz, filtered at 5 kHz) via an ITC-16 A/D board (Instrutech, Long Island, NY, USA) and stored on a Macintosh G4 computer running Axograph v4.6 software (Axon Instruments, Union City, CA, USA). All data were analysed offline using the Axograph software. Subthreshold currents were classified as previously described (Graham *et al.* 2007*c*; Walsh *et al.* 2009). Because the rapid A-type potassium current (I_{Ar}) is the dominant subthreshold current at all developmental stages in mouse lumbar SDH neurons (Walsh *et al.* 2009), its features were analysed further for neonatal and adult mice. I_{Ar} amplitude was measured by subtracting the amplitude of any steady state current component (in the last 50 ms of the step to −40 mV) from the maximal I_{Ar} current peak (Graham *et al.* 2008). Activation and steady state inactivation curves were generated and subsequently fit with Boltzmann equation: $g/g_{max} = 1/[1 + \exp((V - V_{50})/k)]$ where g/g_{max} is normalized conductance, V is membrane potential, V_{50} is voltage at half-maximal activation (or inactivation) for membrane potentials −90 to −40 mV, and k is the slope factor. Under these conditions I_{Ar} is never fully activated, so we could not compare half-activation in the classic sense. We therefore compare data points at each membrane potential (5 mV increments over −90 to −40 mV). The decay phase of the I_{Ar} response was fit with a single exponential (over 20–80% of its falling phase).

Individual APs were captured using a derivative threshold method, with the threshold ranging from 10 to 15 mV ms^{-1} for neonatal neurons, and 18–20 mV ms^{-1} for adult neurons. AP threshold was defined as the inflection point during spike initiation. Rheobase current was defined as the smallest step-current that elicited at least one AP. The amplitude of each AP was measured as the difference between threshold and its maximum positive peak. AP half-width was calculated at 50% of AP amplitude. AP afterhyperpolarization (AHP) amplitude was measured as the difference between AP threshold and its maximum negative peak.

The SPSS v16 software package (SPSS, Chicago, IL, USA) was used for statistical analysis. One-way ANOVA was used to compare means of passive and active properties between/across the three regions of the cord and between neonatal and adult mice. Scheffe's *post hoc* tests were used to determine where data differed. Data that failed Levene's test of homogeneity of variance were compared using the non-parametric Kruskal–Wallace test, followed by Tamhane's T2 *post hoc* test. *G* tests, with Williams's correction, were used to determine whether the prevalence of discharge categories, responses to hyperpolarizing steps, and subthreshold currents differed between regions of the cord and between neonatal and adult mice. Statistical significance was set at $P < 0.05$ and all data are presented as means ± SEM.

Results

Whole cell patch clamp recordings were obtained from over 600 SDH neurons: i.e. ∼100 neurons in the upper cervical, thoracic and lumbar spinal cord regions for both neonate and adult mice (Table 1). Some previously published data for neonatal and adult lumbar SDH neurons were reanalysed and included in this sample (Walsh *et al.* 2009). The location of recorded neurons for each spinal region in neonates and adults is presented in Fig. 1 and suggests recordings were obtained predominantly from neurons in lamina II. It should be noted, however, that the distinction between laminae I and II on our figure is an approximation as these boundaries are not distinct in mice, especially in fresh slices (Woodbury *et al.* 2000; Graham *et al.* 2003). In neonates, recordings were concentrated in the medial SDH because the nearby dorsal columns serve as a guide for confident identification of the grey/white matter border. In contrast, the lateral border of the SDH is not distinct in neonatal cords. Recordings

Table 1. Passive and action potential properties of SDH neurons from different spinal regions in neonates and adults

	Spinal cord region (*n*)	R_{IN} (MΩ)	RMP (mV)	Rheobase current (pA)	AP threshold (mV)	AP height (mV)	AP half-width (ms)	AHP amplitude (mV)
Neonate	C2–C4 (101)	711 ± 41	−58.4 ± 1.0	48 ± 4.0	−38.3 ± 0.5	29.5 ± 1.4	2.29 ± 0.1	−11.5 ± 1.0
	T8–T10 (99)	819 ± 52*	−56.2 ± 1.0*	48 ± 4.0	−39.3 ± 0.5	29.8 ± 1.5	2.47 ± 0.1	−9.5 ± 0.9
	L3–L5 (101)	582 ± 29*	−57.2 ± 0.9	55 ± 5.3*	−38.4 ± 0.5	30.2 ± 1.5	2.28 ± 0.1	−10.4 ± 0.9
Adult	C2–C4 (109)	425 ± 20	−65.7 ± 1.0	77 ± 8.3	−38.3 ± 0.7	49.5 ± 1.2	0.72 ± 0.02	−37.1 ± 0.7
	T8–T10 (108)	429 ± 22	−68.7 ± 1.1	107 ± 11	−39.6 ± 0.5	48.5 ± 1.2	0.70 ± 0.02	−36.8 ± 0.7
	L3–L5 (113)	423 ± 17	−67.4 ± 1.0	89 ± 8.6	−38.8 ± 0.6	47.7 ± 1.3	0.90 ± 0.05	−35.1 ± 0.8

All values except AP threshold differ in neonate and adult SDH neurons. *Difference across spinal regions (see text for more details).

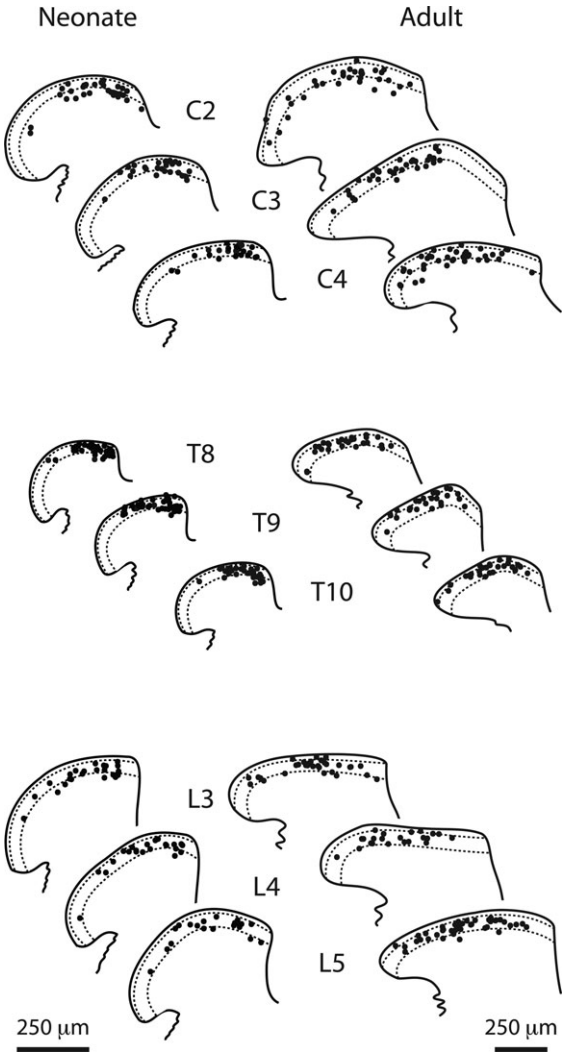

Figure 1. Location of recorded SDH neurons in different spinal regions in neonate and adult mice
The location of each recorded neuron is plotted on one of three templates of the SDH for consecutive spinal segments in the upper cervical (C2–4), thoracic (T8–10) and lumbar (L3–5) cord. Note, the plots for neonatal SDH are shown at higher magnification to facilitate comparison of recorded neuron location between neonates (left) and adults (right).

in adult neurons were spread more evenly across the mediolateral extent of the SDH in each region.

Membrane and action potential properties

Results for passive and active membrane properties for SDH neurons across different spinal regions in neonates and adults are provided in Table 1. When these properties were compared across spinal regions they were remarkably similar in neonatal and adult datasets. Significant differences, however, were observed along the rostro-caudal gradient of the spinal cord for R_{IN} and rheobase current in neonates. Passive membrane properties differed substantially between neonatal and adult neurons: R_{IN} was higher and RMP was ∼10 mV more depolarized in neonatal *versus* adult neurons. Measurements made on rheobase APs showed all properties, except AP threshold, differed between neonate and adult neurons: rheobase current, AP amplitude and AHP amplitude were smaller, whereas AP half-width was greater in neonates.

Responses to depolarizing current injection

We next compared the response of SDH neurons to depolarizing current steps of increasing amplitude across spinal regions in neonates and adults (Fig. 2). Previously, we have shown that responses in mouse lumbar SDH neurons can be assigned to one of five categories (hereafter termed AP discharge categories; Fig. 2*A*) in both slices and *in vivo* (Graham *et al.* 2004, 2007*c*). These AP discharge categories include tonic firing, where AP discharge lasts for the entire duration of the current step; initial bursting, where APs discharge is restricted to the onset of current injection; delayed firing, where AP discharge occurs after a delay from current onset; single spiking, where AP discharge is limited to one, or sometimes two, APs at the onset of the current injection regardless of current intensity; and reluctant firing, where AP discharge is absent in response to current injection. Importantly, reluctant firers were not simply unhealthy neurons as they had similar R_{IN} and RMP to other neurons that discharged APs, and would discharge APs when their membrane

potential was altered (using bias current) to less negative potentials and repeated step current injection (Graham *et al.* 2007*b*).

All five discharge categories were observed in the three spinal regions in both neonates and adults. For neonates, the distribution of discharge categories across the spinal regions was statistically similar ($P = 0.4$; Fig. 2*B*). There were, however, subtle differences in the proportions of some categories. For example, the incidence of single spikers increased caudally (32% *vs.* 48%; upper cervical *vs.* lumbar regions). This was accompanied by the decreased prevalence of initial bursters (35% *vs.* 26%; upper cervical *vs.* lumbar). Similar proportions of tonic firers (∼10%) and reluctant firers (15–20%) were observed across all three regions. Delayed firers were rarely observed in neonates (less than 3% at all levels). In contrast, the distribution of discharge categories in adult neurons differed across spinal regions ($P < 0.05$; Fig. 2*C*). Most notably, the distribution of discharge categories differed between the upper cervical and lumbar regions ($P < 0.05$).

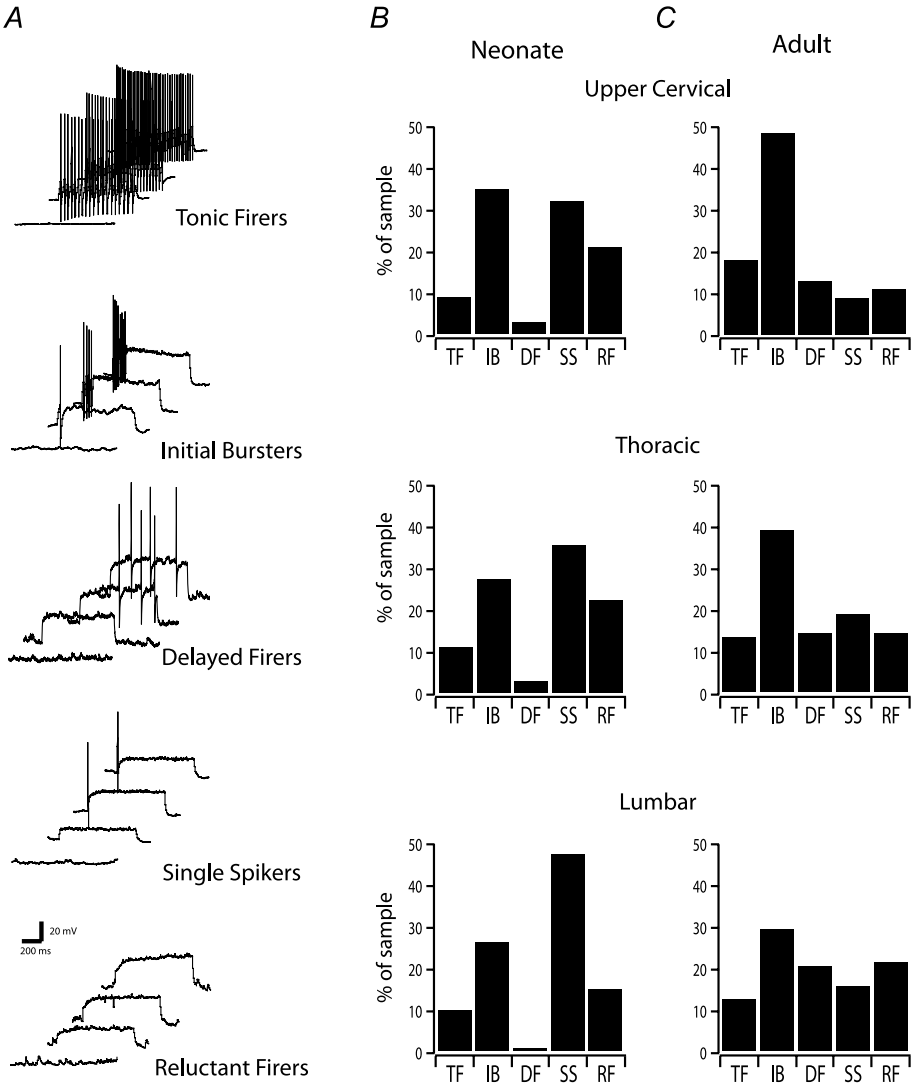

Figure 2. Prevalence of AP discharge categories across spinal regions in neonate and adult SDH neurons
A, representative traces show the five types of AP discharge observed in SDH neurons. All traces are from adult upper cervical neurons, and show responses to increasing amplitude current injections (0, 40, 80 and 120 pA; 800 ms duration). *B*, bar plots showing the prevalence of the five discharge categories for each spinal cord region in neonates. Comparison of the distributions across segments showed they were similar (G statistic = 7.9, $P = 0.4$). *C*, bar plots showing the prevalence of the five discharge categories for each spinal cord region in adults. Comparison of the distributions across segments showed they differed (G statistic = 16.3, $P < 0.05$). Pairwise comparisons revealed upper cervical and lumbar distributions differed (G statistic = 14.6, $P < 0.05$). Comparisons between neonates and adults also revealed significant differences in the distributions in each spinal region (upper cervical G statistic = 27.6, $P < 0.05$; thoracic G statistic = 19.6, $P < 0.05$; lumbar G statistic = 43.9, $P < 0.05$).

The prevalence of initial bursters decreased caudally (48% *vs.* 28%; upper cervical *vs.* lumbar regions), whereas the prevalence of delayed firers (13% *vs.* 21%), single spikers (11% *vs.* 15%), and reluctant firers (10% *vs.* 22%) increased in lumbar regions. Tonic firers comprised ∼15% of the sample in all three spinal regions.

In terms of development, there were marked differences in the distribution of AP discharge patterns between neonatal and adult SDH neurons ($P < 0.05$; Fig. 2*B* *vs.* Fig. 2*C*). Irrespective of spinal region, the prevalence of initial bursters and delayed firers increased, single spikers decreased and the prevalence of both tonic and reluctant firers did not change in neonates compared to adults.

Membrane and action potential properties within discharge categories

As SDH neurons are clearly heterogeneous, based on their response to current injection, we next examined the data presented in Table 1 when divided according to discharge category. These data are shown in Table 2. Overall this exercise showed there are virtually no differences in the selected properties for each discharge category along the rostrocaudal axis of the cord in either neonates or adults. The only difference we noted was for single spikers in neonates: input resistance was higher in neurons from thoracic segments. The developmental differences between neonates and adults (see Table 1) were again evident when the data were compared within discharge categories. Note this analysis was limited in some categories because of their low prevalence (e.g. delayed firers). This additional analysis allows us to confidently state that the various parameters measured are similar across spinal cord regions in both neonates and adults.

Responses to hyperpolarizing current injection

Injection of hyperpolarizing step currents revealed three types of responses, at the end of the current step, in SDH neurons (Graham *et al.* 2004). These are shown in Fig. 3*A*. Rebound responses showed a pronounced depolarization at the end of the current step, which often resulted in AP discharge. Hyperpolarizing responses were characterized by a long-lasting membrane hyperpolarization after cessation of the current step. A third group showed passive responses where the membrane potential returned to resting values according to the membrane time constant of the neuron.

The prevalence of these hyperpolarizing responses in different spinal regions for neonates and adults is shown in Fig. 3*B* and *C*. Overall the distributions, across spinal regions, were statistically similar for both neonates and adults ($P = 0.07$ and 0.2, respectively). However, like the responses to depolarizing steps, some subtle differences existed. In neonates, the prevalence of rebound depolarization decreased caudally (30% *vs.* 21%; upper cervical *vs.* lumbar), although a greater proportion of these neurons failed to discharge APs during rebound depolarization in upper cervical regions (24/30 neurons) compared to thoracic (12/22) and lumbar (10/21) regions. The proportion of neonatal neurons showing sustained hyperpolarization increased caudally (17% *vs.* 28%; upper cervical *vs.* lumbar). Passive responses to hyperpolarizing current injection were observed in ∼50% of neurons from all three regions in neonatal neurons. In adult neurons, rebound depolarization was more prevalent in rostral spinal regions (34% *vs.* 21%; upper cervical *vs.* lumbar). Neurons showing sustained hyperpolarization increased caudally (16% *vs.* 20%; upper cervical *vs.* lumbar). Passive responses dominated in all three regions of the cord (50–65%). Comparison of neonatal and adult responses to hyperpolarizing current steps revealed developmental changes in upper cervical and thoracic regions ($P < 0.05$), but not in the lumbar region ($P = 0.4$). In the upper cervical region the incidence of rebound responses that produced AP discharge increased during development (6% *vs.* 24%), whereas the prevalence of passive responses increased (52% *vs.* 65%) in thoracic regions.

Close examination of hyperpolarization responses, during current step injection, showed only a few neurons exhibited the classical H-current 'sag' as observed in motor neurons, for example. In neonatal neurons sag was observed in 5–10% of the cells in all three spinal regions. For adults, this was 6–8% and was similar in all regions.

Where numbers permitted, we examined whether there was any correlation between the responses to hyperpolarizing current injection and firing pattern. In adult neurons tonic firers, initial bursters and single spikers exhibited similar proportions of rebound, hyperpolarizing and passive responses to hyperpolarizing current. In contrast, delayed firers and reluctant firers rarely exhibited the rebound response. These patterns were similar along the length of the spinal cord. Similar responses were observed in neonates, but the relationships for delayed firers could not be determined because of their low prevalence in neonates.

As rapid A (I_{Ar}), is the dominant current in SDH neurons (see next section) we examined whether this current correlated with responses to hyperpolarizing current injection. Virtually all cells (66/67) with a hyperpolarizing response exhibited the I_{Ar} current in neonates. In adults, almost all (50/52) neurons with the hyperpolarizing response exhibited either rapid (I_{Ar}) or slow A (I_{As}) currents. Importantly, these relationships did not differ across spinal regions.

Table 2. Membrane and action potential properties for SDH neurons according to action potential discharge category in neonates and adults

Discharge category	Age	Region	*n*	Input resistance (MΩ)	Capacitance (pF)	RMP (mV)	Rheobase current (pA)	AP threshold (mV)	AP amplitude (mV)	AP half-width (ms)	AHP amplitude (mV)
Tonic firers	Neonate	C2–C4	9	574 ± 55	20.4 ± 0.9	−67.4 ± 2.3	33 ± 7.5	−38.8 ± 1.5	41.1 ± 2.8	1.29 ± 0.11	−21.4 ± 1.5
		T8–T10	11	594 ± 106	22.9 ± 2.8	−63.4 ± 2.2	29 ± 6.2	−42.8 ± 1.1	42.6 ± 5.9	1.76 ± 0.24	−16.4 ± 1.7
		L3–L5	11	594 ± 79	20.2 ± 3.1	−61.3 ± 2.8	29 ± 4.1	−41.2 ± 2.1	46.7 ± 4.6	1.37 ± 0.16	−19.6 ± 1.7
	Adult	C2–C4	20	391 ± 39	14.2 ± 1.1	−61.4 ± 1.1	27 ± 2.6	−39.7 ± 0.8	53.0 ± 2.5	0.65 ± 0.02	−40.5 ± 1.2
		T8–T10	16	398 ± 49	14.9 ± 1.2	−66.0 ± 1.7	33 ± 4.0	−40.3 ± 1.0	56.9 ± 1.6	0.61 ± 0.03	−40.5 ± 2.0
		L3−L5	15	389 ± 44	16.4 ± 1.6	−61.1 ± 1.9	31 ± 6.7	−41.0 ± 0.9	55.0 ± 3.0	0.91 ± 0.12	−35.2 ± 2.4
Initial bursters	Neonate	C2–C4	35	657 ± 62	21.4 ± 1.1	−59.9 ± 1.4	32 ± 2.5	−39.2 ± 0.9	35.8 ± 1.8	1.99 ± 0.15	−15.4 ± 1.3
		T8–T10	27	739 ± 53	21.1 ± 1.2	−60.6 ± 1.1	34 ± 4.1	−40.0 ± 0.7	35.4 ± 1.9	1.93 ± 0.13	−13.7 ± 1.2
		L3–L5	26	517 ± 35	19.7 ± 1.4	−62.3 ± 1.6	45 ± 11.9	−39.9 ± 0.8	36.8 ± 2.7	1.66 ± 0.12	−14.4 ± 1.5
	Adult	C2–C4	52	421 ± 27	17.4 ± 0.9	−63.2 ± 1.4	58 ± 8.1	−38.1 ± 1.1	52.5 ± 1.4	0.74 ± 0.03	−36.2 ± 0.9
		T8–T10	38	453 ± 39	15.0 ± 0.9	−63.1 ± 1.4	64 ± 9.9	−38.8 ± 0.9	48.9 ± 1.9	0.73 ± 0.03	−37.7 ± 1.1
		L3–L5	32	391 ± 31	15.5 ± 0.9	−61.7 ± 1.5	65 ± 10.5	−38.6 ± 1.0	48.7 ± 1.9	0.88 ± 0.09	−34.7 ± 1.3
Delayed firers	Neonate	C2–C4	3	569 ± 50	30.0 ± 6.6	−64.9 ± 2.2	80 ± 50	−35.5 ± 1.5	23.5 ± 4.9	1.99 ± 0.30	−11.9 ± 3.4
		T8–T10	3	610 ± 275	18.3 ± 6.8	−77.5 ± 2.4	120 ± 20	−38.7 ± 3.4	29.3 ± 2.2	1.83 ± 0.15	−17.0 ± 4.2
		L3–L5	1	743	22.9	−66.4	40	−37.7	29.3	1.82	−20.6
	Adult	C2–C4	14	580 ± 83	21.1 ± 1.8	−74.7 ± 1.9	147 ± 26	−35.2 ± 1.3	41.0 ± 4.0	0.68 ± 0.03	−37.7 ± 1.2
		T8–T10	16	513 ± 54	20.1 ± 1.7	−75.8 ± 2.5	135 ± 24	−38.5 ± 1.2	47.3 ± 2.7	0.74 ± 0.04	−36.6 ± 1.3
		L3–L5	24	483 ± 25	18.7 ± 1.5	−72.8 ± 1.4	128 ± 19	−37.2 ± 1.0	44.8 ± 2.1	0.94 ± 0.09	−37.9 ± 1.3
Single spikers	Neonate	C2–C4	32	661 ± 69	21.0 ± 1.3	−55.7 ± 1.4	68 ± 7	−37.5 ± 0.8	19.9 ± 1.3	2.94 ± 0.21	−4.5 ± 1.0
		T8–T10	35	819 ± 94*	21.0 ± 1.0	−54.9 ± 1.0	57 ± 7	−37.9 ± 0.9	21.7 ± 1.1	3.16 ± 0.20	−3.1 ± 1.1
		L3–L5	47	523 ± 42	21.9 ± 1.0	−55.6 ± 1.1	67 ± 7	−37.1 ± 0.7	22.6 ± 1.1	2.90 ± 0.21	−5.4 ± 1.0
	Adult	C2–C4	12	353 ± 54	15.7 ± 1.5	−63.7 ± 2.4	162 ± 32	−40.4 ± 1.6	40.7 ± 3.2	0.75 ± 0.09	−34.3 ± 2.8
		T8–T10	18	344 ± 38	15.9 ± 1.3	−69.8 ± 1.5	224 ± 28	−41.9 ± 1.3	43.8 ± 2.5	0.68 ± 0.05	−31.8 ± 1.4
		L3–L5	17	401 ± 50	16.6 ± 1.4	−61.9 ± 1.7	132 ± 21	−38.5 ± 1.4	45.4 ± 3.4	0.86 ± 0.08	−32.3 ± 2.1
Reluctant firers	Neonate	C2–C4	21	919 ± 123	19.0 ± 1.5	−55.3 ± 3.0					
		T8–T10	22	1072 ± 142	19.3 ± 1.3	−45.9 ± 1.9					
		L3–L5	15	818 ± 112	18.4 ± 2.1	−49.9 ± 1.9					
	Adult	C2–C4	11	383 ± 42	20.9 ± 1.9	−76.2 ± 1.7					
		T8–T10	13	411 ± 83	21.3 ± 1.8	−77.3 ± 4.5					
		L3–L5	25	440 ± 42	22.3 ± 1.7	−77.2 ± 1.9					

*Difference within spinal region.

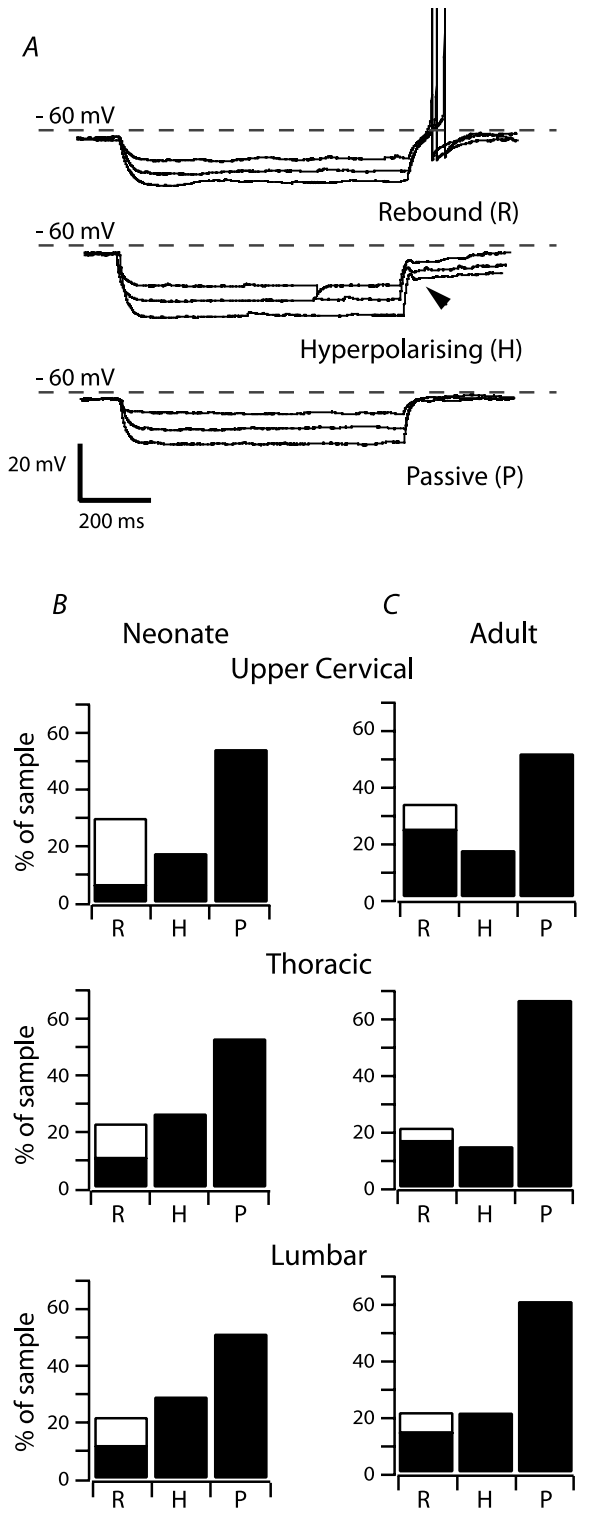

Figure 3. Prevalence of responses to hyperpolarizing current injection across spinal regions in neonate and adult SDH neurons
A, representative traces show three responses to hyperpolarizing current injection in SDH neurons. All traces are from adult upper cervical neurons and show responses to increasing amplitude current injections (−20, −30 and −40 pA; 800 ms duration). Dashed line indicates membrane potential of −60 mV. *B*, bar plots showing the prevalence of responses to hyperpolarizing current injection for each spinal cord region in neonates. Note the rebound responses are separated for neurons that discharge an AP (filled) and those that did not (open). Comparison of the distributions across segments showed they were similar (G statistic = 11.7, $P = 0.07$). *C*, bar plots showing the prevalence of the responses to hyperpolarizing current injection for each spinal cord region in adults. Comparison of the distributions across segments showed they were similar (G statistic = 8.3, $P = 0.2$). Comparisons between neonates and adults revealed significant differences in the distributions in upper cervical and thoracic but not lumbar spinal regions (upper cervical G statistic = 18.4, $P < 0.05$; thoracic G statistic = 9.9, $P < 0.05$; lumbar G statistic = 2.8, $P = 0.4$).

Subthreshold currents

Data for subthreshold currents were obtained in 597/631 of the recorded neurons: 280/301 neonatal and 317/330 adult neurons (Fig. 4). The vast majority of the neurons (88% for neonates and 79% for adults) exhibited a single subthreshold current in response to our protocol: either rapid A (I_{Ar}), slow A (I_{As}), the non-specific cation current (I_H) or the T-type calcium current (I_{Ca}). The remaining neurons exhibited combinations of subthreshold currents, which we term 'mixed' subthreshold currents.

The expression of the various subthreshold currents across the three spinal regions was remarkably similar in both neonatal and adult SDH neurons ($P = 0.7$ and 0.4, respectively; Fig. 4*B* and *C*). In neonatal SDH neurons, I_{Ar} was the dominant subthreshold current in all spinal regions accounting for ∼80% of the sample. I_{As} was not observed in any spinal region and I_H, I_{Ca}, or mixed currents never accounted for more than 15% of the sample in any spinal region. In adult neurons, I_{Ar} was the dominant subthreshold current, but the prevalence of I_{Ar} increased in caudal spinal regions (42% *vs.* 59%; upper cervical *vs.* lumbar). I_{As}, I_{Ca}, or mixed currents accounted for the remainder, with each comprising <20% of the sample. I_H was rarely encountered (∼2%) in any spinal region. The mean amplitude of each subthreshold current did not differ across spinal regions in either neonates or adults. Comparison of the prevalence of subthreshold currents during development showed significant changes in the three spinal regions ($P < 0.05$). The most notable difference was a decreased expression of I_{Ar} (by ∼20%) and increased expression of I_{As} to 15–20% during development.

Properties of the rapid A (I_{Ar}) current

Because I_{Ar} is the dominant current in both neonatal and adult SDH neurons we undertook a detailed analysis of its properties and these data are shown in Table 3. Generally, values were similar across spinal regions for both neonates and adults. In neonates, upper cervical neurons had faster

inactivation kinetics and the amplitude of the steady state current was reduced in thoracic neurons. Several properties of I_{Ar}, however, differed substantially in neonate *versus* adult neurons in all spinal regions: specifically, peak and steady state current amplitude were smaller, whereas inactivation was faster (Table 3).

We next compared the activation and steady state inactivation of I_{Ar} across spinal regions for neonatal and adult neurons (Fig. 5). For neonates, activation plots were identical across spinal cord regions (Fig. 5*A*). In contrast, the steady state inactivation was shifted to the left for upper cervical neurons at potentials between −70 and −60 mV. Similar analysis of activation and steady state inactivation on adult neurons showed activation differed slightly in lumbar neurons at membrane potentials between −55 and −50 mV (Fig. 5*B*). The steady state inactivation was shifted to the right for upper cervical neurons at potentials between −80 and −60 mV.

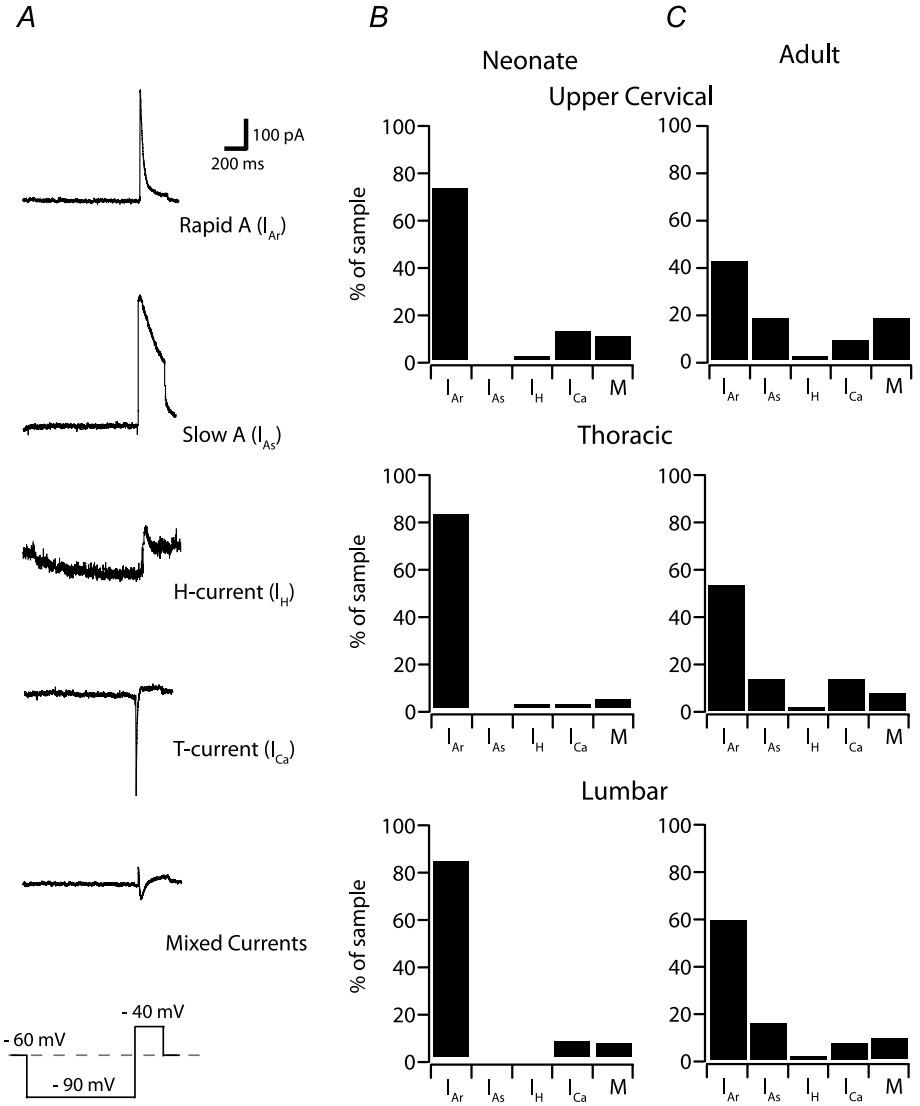

Figure 4. Prevalence of subthreshold currents across spinal regions in neonate and adult SDH neurons
A, representative traces show the five subthreshold currents observed in SDH neurons. The illustrated mixed current consists of an outward A-current and an inward T-current. Bottom trace shows voltage protocol used to activate the above currents from a holding potential of −60 mV. All traces are from adult upper cervical neurons. *B*, bar plots showing the prevalence of subthreshold currents for each spinal cord region in neonates. Comparison of the distributions across segments showed they were similar (G statistic = 6.0, $P = 0.7$). *C*, bar plots showing the prevalence of subthreshold currents for each spinal region in adults. Comparison of the distributions across segments showed they were similar (G statistic = 8.5, $P = 0.4$). Comparisons between neonates and adults revealed significant differences in the distributions in each spinal region (upper cervical G statistic = 19.5, $P < 0.05$; thoracic G statistic = 16.3, $P < 0.05$; lumbar G statistic = 12.9, $P < 0.05$).

Table 3. Properties of the I_{Ar} subthreshold current in SDH neurons from different spinal regions in neonates and adults

	Spinal cord region (*n*)	Peak amplitude (pA)	Decay time constant (ms)	Steady state current (pA)
Neonate	C2–C4 (68)	173.0 ± 19.1	17.2 ± 1.5*	16.9 ± 2.5
	T8–T10 (75)	150.8 ± 18.0	22.4 ± 2.1	11.7 ± 1.5*
	L3–L5 (80)	159.0 ± 14.0	26.3 ± 2.6	14.3 ± 2.1
Adult	C2–C4 (44)	300.8 ± 47.1	35.6 ± 5.1	69.2 ± 14.0
	T8–T10 (55)	359.1 ± 40.9	45.8 ± 4.5	54.7 ± 11.8
	L3–L5 (64)	346.3 ± 39.0	38.8 ± 3.5	45.3 ± 5.5

All values differ in neonate and adult neurons. *Difference across spinal regions (see text for more details).

In addition, there were clear differences in I_{Ar} activation and steady state inactivation between neonate and adult neurons (Fig. 5*C–E*). In the upper cervical sample, activation of I_{Ar} was shifted slightly to the right in neonates at −50 and −45 mV whereas steady state inactivation was shifted markedly to the left for neonatal neurons at potentials between −80 and −60 mV (Fig. 5*C*). In the thoracic sample, both activation and steady state inactivation were identical in neonates and adults (Fig. 5*D*). In the lumbar sample, I_{Ar} activation was shifted to the right in neonates for potentials between −55 and −45 mV, whereas steady state inactivation was identical (Fig. 5*E*). Together these data suggest I_{Ar} kinetics in SDH neurons differ slightly in the upper cervical cord, but markedly between neonates and adults.

Discussion

This study was driven by two considerations that are important for understanding spinal pain mechanisms. First, most of what we know about the intrinsic properties of SDH neurons comes from studies in lumbar segments of the spinal cord. This view overlooks clinical evidence, which suggests processing of nociceptive signals from viscera and structures in the head and neck differs from those in the hindlimb. Second, there is increasing evidence that nociceptive signals are processed differently in the spinal cords of neonates and adults and little developmental data exists for regions outside the lumbar cord.

Limitations of this study

There is a possibility that the differing prevalence of firing patterns and other properties in neonates and adults may be a consequence of the different methods of anaesthesia (i.e. hypothermia *versus* ketamine). Ketamine binds to NMDA receptors and is often used for slice preparation, especially in older animals, because it prevents excitotoxicity associated with glutamate release that follows decapitation (de Oliveira *et al.* 2010). Electrophysiological studies have, however, shown that *direct* ketamine application in neurons may decrease firing frequency, via inhibition of Na^+ and K^+ channels (Schnoebel *et al.* 2005). An increase in input resistance and inhibition of excitatory postsynaptic potentials (EPSPs) has also been associated with direct application of ketamine (Leong *et al.* 2004). Importantly, such action occurs during application of ketamine with these properties returning to control levels within minutes after removal of the drug. Thus, we don't believe method of anaesthesia was a confound in our experiments as ketamine would have washed out of the slices by the time recordings were made.

Processing mechanisms in different regions of the adult spinal cord

Overall our data show that one of the major contributors to signal processing in the SDH (i.e. a neuron's intrinsic membrane properties) is generally conserved in SDH neurons along the length of the spinal cord. Values for R_{IN}, RMP and selected AP properties do not vary along the rostrocaudal axis of the adult spinal cord (Tables 1 and 2). Moreover, the discharge categories described previously in lumbar SDH neurons in deeply anaesthetized rodents (Graham *et al.* 2004), acute slices (Prescott & De Koninck, 2002; Ruscheweyh & Sandkuhler, 2002; Melnick, 2011) or organotypic cultures (Lu *et al.* 2006) are represented in the three spinal cord regions we examined. These data suggest the relative constancy in the electrophysiological properties and discharge heterogeneity is fundamental to the way SDH neurons process peripheral signals, regardless of their source.

One possible explanation for the relative constancy in the intrinsic properties of SDH neurons along the spinal cord is that it provides a 'stable base' upon which peripheral synaptic inputs, with differing properties, determine neuron output. Indeed, there is evidence for differences in peripheral input to upper cervical, thoracic and lumbar cord. For example, in the upper cervical cord SDH neurons receive input from a unique combination of tissues including cutaneous and deep structures in the neck, head and cranial vault (Morch *et al.* 2007; Olesen *et al.* 2009), and even the heart (Foreman, 1999). This afferent convergence from varied sources presumably

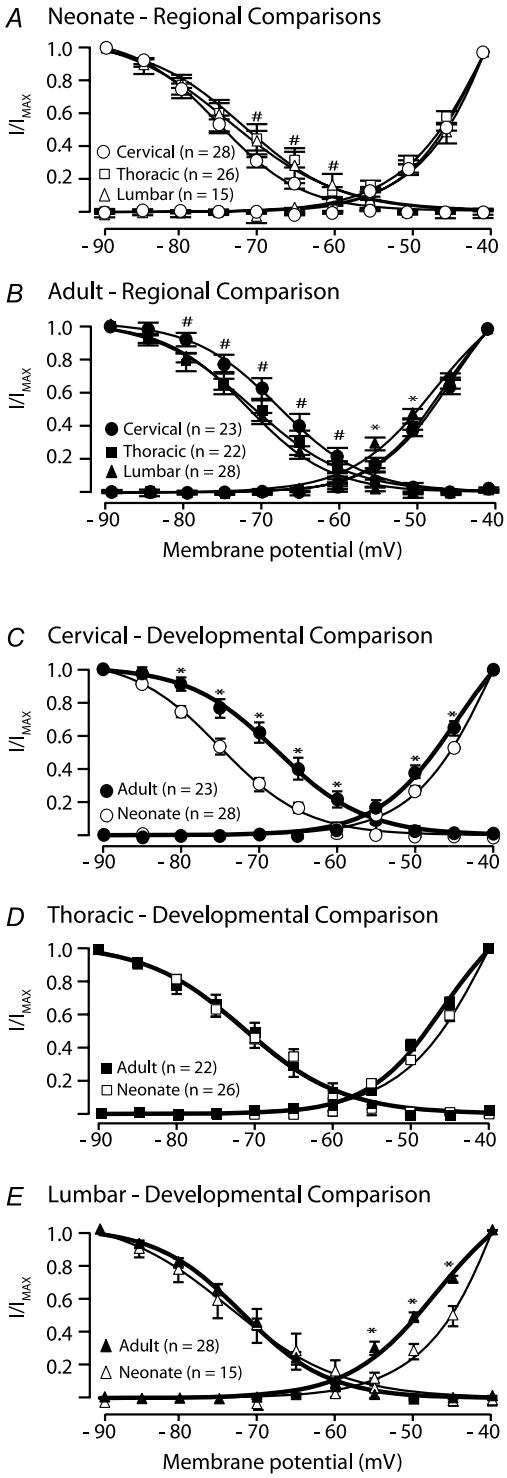

Figure 5. Regional and developmental comparisons of IAr activation and steady state inactivation.
A-B, plots comparing activation and steady-state inactivation of IAr across spinal regions in neonates (A) and adults (B) at membrane potentials between −90 and −40 mV. C–E, plots comparing activation and steady-state inactivation of IAr between neonates and adults in upper cervical (C), thoracic (D) and lumbar spinal cord (E) at membrane potentials between −90 and −40 mV. Asterisks indicate differences ($P < 0.05$) in pairwise comparisons for data points at various membrane potentials.

plays an important role in the complex presentation of pain originating in orofacial and neck tissues (Hu *et al.* 2005). Likewise, many afferents entering the thoracic cord originate in viscera and are known to differ in their innervation density, neurotransmitter phenotype, and sensitivity to various types of stimuli (Cervero, 1994; Gebhart & Bielefeldt, 2009).

While little information exists on the electrical properties of dorsal root ganglia (DRGs) outside lumbosacral regions of the cord there are clear anatomical differences between DRGs that project to skin, muscle or viscera. Those innervating viscera are larger than their somatic counterparts (Neuhuber *et al.* 1986; Perry & Lawson, 1998) and differ in the expression of various peptides (McMahon *et al.* 1994; Bennett *et al.* 1996; Lu *et al.* 2001; Lawson, 2005). Differences in rostrocaudal location has also been advanced as an explanation for the variation in percentages of neurons that are positive for various neurochemical markers (Lawson, 2005). Together these data suggest the anatomical and chemical properties of somatic and visceral DRGs differ to reflect the peripheral target they innervate.

There is also some evidence for differences in the way the central terminals of peripheral afferents from skin, muscle, joints or viscera terminate and branch in the dorsal horn. Anatomical studies have shown that electrophysiologically identified cutaneous afferents exhibit a dense and focused branching pattern in lamina I–II (Sugiura *et al.* 1986). This suggests cutaneous afferents exert a powerful effect on a limited number of SDH neurons. In contrast, the central terminals of similarly labelled visceral afferents have sparse and widely distributed terminal fields: over multiple laminae (I–II, IV and X) and spinal segments (Sugiura *et al.* 1989). No equivalent data are available for afferents from muscle and joints. In summary, the available evidence suggests differences in the organization of peripheral inputs to the dorsal horn could, in part, explain the reported regional differences in pain processing mechanisms.

Functional significance of initial bursting in upper cervical segments

Significantly more initial bursting neurons were present in rostral segments of the cord (Fig. 2). Studies on medullary (brainstem) dorsal horn neurons also report a high prevalence of initial bursting (Davies & North, 2009). Thus, initial bursting may play a dominant role in signal processing in rostral regions of the pain neuroaxis. Several groups have shown that certain discharge profiles are associated with specific neurochemical phenotypes in lumbosacral cord (Todd, 2010). Tonic firing neurons are often inhibitory (Lu & Perl, 2003; Heinke *et al.* 2004; Labrakakis *et al.* 2009; Yasaka *et al.* 2010), whereas delayed

firing neurons are excitatory (Biggs *et al.* 2010; Yasaka *et al.* 2010). Such relationships have not been demonstrated for initial bursting neurons. Thus at this stage they cannot be assigned an excitatory or inhibitory role in signal processing.

A number of groups have suggested discharge heterogeneity in the SDH allows neurons to code stimulus properties such as intensity and duration (tonic firing and initial bursting), novelty (single spiking) and history of excitation (delayed and reluctant firing) (Prescott & De Koninck, 2002; Ruscheweyh & Sandkuhler, 2002; Melnick *et al.* 2004). The dominance of initial bursting neurons in upper cervical segments would provide the upper cervical cord with a capacity to code stimulus intensity and duration, as well as generate APs more readily than their counterparts in thoracic and lumbar regions. We have shown previously that the distinction between tonic firing and initial bursting blurs into a single discharge category when lumbar SDH neurons are activated by current profiles that more closely resemble synaptic activation (Graham *et al.* 2007*b*). If this were the case for upper cervical neurons, then tonic firing and initial bursting would form a major discharge category (∼70% of neurons) and dominate signal processing in the upper cervical cord.

Developmental differences

Like adult SDH neurons, there is a remarkable conservation of passive and active membrane properties across spinal segments in neonatal SDH neurons (Tables 1 and 2 and Figs 2–4). Single spiking dominates, delayed firing is rarely observed, and I_{Ar} is the most prevalent subthreshold current in young neurons. Approximately 80% of neonatal SDH neurons in each spinal region expressed the I_{Ar} potassium current, and its kinetics varied little across segments (Figs 4, 5). These observations suggest a similar developmental programme initially establishes intrinsic properties in SDH neurons independent of their rostrocaudal location in the spinal cord.

There are, however, marked differences in the properties of SDH neurons in the neonatal and adult spinal cord. For all regions R_{IN} decreases, RMP becomes more hyperpolarized (by ∼10 mV), and the proportions of the various discharge categories and subthreshold currents change markedly between P0–5 and P24–45 (Figs 2–4). These data are consistent with a recent study by our group, in mouse lumbar cord, which showed that P0–5 and >P25 represent periods where the intrinsic properties of SDH neurons differ most during postnatal development (Walsh *et al.* 2009). For lumbar cord, we know that these changes in intrinsic properties are accompanied by considerable synaptic remodelling during development (Fitzgerald *et al.* 1994; Mirnics & Koerber, 1995; Coull *et al*, 2003; Baccei & Fitzgerald, 2004). No comparable data are available for the development of synaptic inputs that arise in deep structures, like axial muscles in the neck or from viscera. However, studies that have examined behavioural and physiological consequences of visceral insults during early postnatal development suggest synaptic mechanisms may also be very plastic in these spinal regions in the neonate. For example, neonatal, but not adult, exposure to lipopolysaccharide (LPS) produces long-term exacerbations in the development of colitis in adults (Spencer *et al.* 2007). Likewise, colon irritation in neonates, but not in adults, results in chronic visceral hypersensitivity (Al-Chaer *et al.* 2000). These studies on visceral targets thus produce similar results to those observed following inflammation in the limbs. Here peripheral inflammation during the neonatal period can have long-standing consequences on the development of nociceptive circuitry whereas similar interventions in the third postnatal week fail to do so (Ruda *et al.* 2000; Li & Baccei, 2009). Together these data suggest the ability of tissue injury to modulate synaptic function in SDH neurons differs in the neonatal and mature spinal cord and that similar mechanisms operate in regions of the cord that receive input from viscera.

I_{Ar} potassium current function across segments and during development

The I_{Ar} type potassium current is the dominant subthreshold current in both neonatal and adult mouse SDH neurons (Fig. 4) and its expression and kinetics remain relatively constant across spinal regions for both age groups (Fig. 5*A* and *B*).

As the I_{Ar} current is thought to suppress excitability and underlie delayed firing (Connor & Stevens, 1971; Hu *et al.* 2007; Melnick, 2011) it is surprising that delayed firing is not the dominant discharge pattern in SDH neurons. In fact, in neonates delayed firing is rarely observed in any spinal region (Fig. 2). A possible explanation lies in the more depolarized RMPs (∼10 mV) in neonatal neurons, i.e. I_{Ar} is less effective at depolarized membrane potentials. In adults delayed firing is more prevalent in caudal spinal regions and is accompanied by increased incidence of I_{Ar}. Combined with the lower RMPs in adult neurons, this observation suggests I_{Ar} is more important in shaping discharge in adult *versus* neonatal SDH neurons.

During development there are marked changes in the properties of the I_{Ar} current in upper cervical and lumbar regions of the cord (Fig. 5*C* and *E*). In the upper cervical cord, I_{Ar} is more inactivated in neonates at membrane potentials between −60 and −80 mV. This would make I_{Ar} less effective at influencing discharge in the upper cervical cord of neonates. There is also a developmental change in the activation of I_{Ar} in the lumbar region in neonates. Effectively, the current activates at more depolarized potentials in this spinal region. Together, these

two findings provide additional mechanisms that render I_{Ar} less influential in the neonate and help explain the low incidence of delayed firing during early development.

The changes in I_{Ar} properties in upper cervical and lumbar neurons during development (Fig. 5*C* and *E*) suggest different mechanisms shape I_{Ar} expression along the rostrocaudal axis of the spinal cord during development. Indeed, recent evidence shows this current is subject to selective expression and modulation in adult SDH neurons. For example, selective expression of Kv4.2-containing subunits underlies the different activation and steady state inactivation properties of I_{Ar} in excitatory and inhibitory SDH neurons (Hu & Gereau, 2011). In addition, activation of a specific metabotropic glutamate receptor (mGluR5) leads to ERK-mediated phosphorylation and modulation of Kv4.2-containing I_{Ar} channels in dorsal horn neurons (Hu *et al.* 2007). Irrespective of mechanisms, the developmental differences in I_{Ar} properties we describe are important as it is becoming increasingly clear that I_{Ar} is highly mutable and often influenced by events resulting in peripheral inflammation or damage to the nervous system (Yoshimura & de Groat, 1999; Hu *et al.* 2006). Moreover, there is evidence that alterations to I_{Ar} function may also be organ, and by inference, spinal region specific (Xu *et al.* 2006).

Conclusions and future directions

Our findings have broad implications for the understanding of processing mechanisms in the SDH. First, the relative constancy of intrinsic membrane properties in SDH neurons in upper cervical, thoracic and lumbar cord means the extensive data collected on the intrinsic properties of SDH neurons in lumbar segments can be applied throughout the rostrocaudal axis of the spinal cord. Second, the existence of relatively constant intrinsic membrane properties provides impetus for testing the hypothesis that the properties of peripheral synaptic inputs shape the differences in nociceptive processing in various regions of the cord. Importantly, one of the major impediments (i.e. short dorsal roots) to studying synaptic inputs to SDH neurons outside the lumber cord can now be overcome by using *in vivo* preparations of the mouse spinal cord (Graham *et al.* 2007*c*). Such preparations allow the application of both electrical and natural stimuli to peripheral nerves and tissues in normal and genetically altered mice.

References

Al-Chaer ED, Kawasaki M & Pasricha PJ (2000). A new model of chronic visceral hypersensitivity in adult rats induced by colon irritation during postnatal development. *Gastroenterology* **119**, 1276–1285.

Andrew D (2009). Sensitization of lamina I spinoparabrachial neurons parallels heat hyperalgesia in the chronic constriction injury model of neuropathic pain. *J Physiol* **587**, 2005–2017.

Baccei ML & Fitzgerald M (2004). Development of GABAergic and glycinergic transmission in the neonatal rat dorsal horn. *J Neurosci* **24**, 4749–4757.

Barnsley L, Lord S & Bogduk N (1994). Whiplash injury. *Pain* **58**, 283–307.

Barry PH & Lynch JW (1991). Liquid junction potentials and small cell effects in patch-clamp analysis. *J Membr Biol* **121**, 101–117.

Bennett DL, Dmietrieva N, Priestley JV, Clary D & McMahon SB (1996). trkA, CGRP and IB4 expression in retrogradely labelled cutaneous and visceral primary sensory neurones in the rat. *Neurosci Lett* **206**, 33–36.

Berberich P, Hoheisel U & Mense S (1988). Effects of a carrageenan-induced myositis on the discharge properties of group III and IV muscle receptors in the cat. *J Neurophysiol* **59**, 1395–1409.

Biggs JE, Lu VB, Stebbing MJ, Balasubramanyan S & Smith PA (2010). Is BDNF sufficient for information transfer between microglia and dorsal horn neurons during the onset of central sensitization? *Mol Pain* **6**, 44.

Cervero F (1994). Sensory innervation of the viscera: peripheral basis of visceral pain. *Physiol Rev* **74**, 95–138.

Cervero F & Connell LA (1984). Distribution of somatic and visceral primary afferent fibres within the thoracic spinal cord of the cat. *J Comp Neurol* **230**, 88–98.

Cervero F & Laird JMA (1999). Visceral pain. *Lancet* **353**, 2145–2148.

Cervero F & Tattersall JE (1987). Somatic and visceral inputs to the thoracic spinal cord of the cat: marginal zone (lamina I) of the dorsal horn. *J Physiol* **388**, 383–395.

Connor JA & Stevens CF (1971). Prediction of repetitive firing behaviour from voltage clamp data on an isolated neurone soma. *J Physiol* **213**, 31–53.

Copp AJ, Greene ND & Murdoch JN (2003). The genetic basis of mammalian neurulation. *Nat Rev Genet* **4**, 784–793.

Coull JA, Boudreau D, Bachand K, Prescott SA, Nault F, Sik A, De Koninck P & De Koninck Y (2003). Trans-synaptic shift in anion gradient in spinal lamina I neurons as a mechanism of neuropathic pain. *Nature* **424**, 938–942.

Daniele CA & MacDermott AB (2009). Low-threshold primary afferent drive onto gabaergic interneurons in the superficial dorsal horn of the mouse. *J Neurosci* **29**, 686–695.

Davies AJ & North RA (2009). Electrophysiological and morphological properties of neurons in the substantia gelatinosa of the mouse trigeminal subnucleus caudalis. *Pain* **146**, 214–221.

de Oliveira RB, Graham B, Howlett MC, Gravina FS, Oliveira MW, Imtiaz MS, Callister RJ, Lim R, Brichta AM & van Helden DF (2010). Ketamine anesthesia helps preserve neuronal viability. *J Neurosci Methods* **189**, 230–232.

Drummond GB (2009). Reporting ethical matters in *The Journal of Physiology*: standards and advice. *J Physiol* **587**, 713–719.

Fitzgerald M, Butcher T & Shortland P (1994). Developmental changes in the laminar termination of A fibre cutaneous sensory afferents in the rat spinal cord dorsal horn. *J Comp Neurol* **348**, 225–233.

Foreman RD (1999). Mechanisms of cardiac pain. *Annu Rev Physiol* **61**, 143–167.

Gebhart GF & Bielefeldt K (2009). Visceral Pain. In *Science of Pain*, ed. Basbaum AI & Bushnell C, pp. 543–569. Elsevier.

Giamberardino MA (1999). Recent and forgotten aspects of visceral pain. *Eur J Pain* **3**, 77–92.

Graham BA, Brichta AM & Callister RJ (2004). In vivo responses of mouse superficial dorsal horn neurones to both current injection and peripheral cutaneous stimulation. *J Physiol* **561**, 749–763.

Graham BA, Brichta AM & Callister RJ (2007*a*). Moving from an averaged to specific view of spinal cord pain processing circuits. *J Neurophysiol* **98**, 1057–1063.

Graham BA, Brichta AM & Callister RJ (2007*b*). Pinch-current injection defines two discharge profiles in mouse superficial dorsal horn neurones, *in vitro*. *J Physiol* **578**, 787–798.

Graham BA, Brichta AM & Callister RJ (2008). Recording temperature affects the excitability of mouse superficial dorsal horn neurons, in vitro. *J Neurophysiol* **99**, 2048–2059.

Graham BA, Brichta AM, Schofield PR & Callister RJ (2007*c*). Altered potassium channel function in the superficial dorsal horn of the spastic mouse. *J Physiol* **584**, 121–136.

Graham BA, Schofield PR, Sah P & Callister RJ (2003). Altered inhibitory synaptic transmission in superficial dorsal horn neurones in spastic and oscillator mice. *J Physiol* **551**, 905–916.

Heinke B, Ruscheweyh R, Forsthuber L, Wunderbaldinger G & Sandkuhler J (2004). Physiological, neurochemical and morphological properties of a subgroup of GABAergic spinal lamina II neurones identified by expression of green fluorescent protein in mice. *J Physiol* **560**, 249–266.

Hu H-J, Alter BJ, Carrasquillo Y, Qiu C-S & Gereau RW 4th (2007). Metabotropic glutamate receptor 5 modulates nociceptive plasticity via extracellular signal-regulated kinase Kv4.2 signaling in spinal cord dorsal horn neurons. *J Neurosci* **27**, 13181–13191.

Hu H-J, Carrasquillo Y, Karim F, Jung WE, Nerbonne JM, Schwarz TL & Gereau IV RW (2006). The Kv4.2 potassium channel subunit is required for pain plasticity. *Neuron* **50**, 89–100.

Hu HJ & Gereau RW 4th (2011). Metabotropic glutamate receptor 5 regulates excitability and Kv4.2-containing K^+ channels primarily in excitatory neurons of the spinal dorsal horn. *J Neurophysiol* **105**, 3010–3021.

Hu JW, Sun K-Q, Vernon H & Sessle BJ (2005). Craniofacial inputs to upper cervical dorsal horn: Implications for somatosensory information processing. *Brain Res* **1044**, 93–106.

Humphrey T (1969). The relation between human fetal mouth opening reflexes and closure of the palate. *Am J Anat* **125**, 317–344.

Ikeda H, Stark J, Fischer H, Wagner M, Drdla R, Jager T & Sandkuhler J (2006). Synaptic amplifier of inflammatory pain in the spinal dorsal horn. *Science* **312**, 1659–1662.

Jobling P, Graham BA, Brichta AM & Callister RJ (2010). Cervix stimulation evokes predominantly subthreshold synaptic responses in mouse thoracolumbar and lumbosacral superficial dorsal horn neurons. *J Sex Med* **7**, 2068–2076.

Kaube H, Keay KA, Hoskin KL, Bandler R & Goadsby PJ (1993). Expression of c-Fos-like immunoreactivity in the caudal medulla and upper cervical spinal cord following stimulation of the superior sagittal sinus in the cat. *Brain Res* **629**, 95–102.

Kuo DC & de Groat WC (1985). Primary afferent projections of the major splanchnic nerve to the spinal cord and gracile nucleus of the cat. *J Comp Neurol* **231**, 421–434.

Kuo DC, Nadelhaft I, Hisamitsu T & de Groat WC (1983). Segmental distribution and central projections of renal afferent fibers in the cat studied by transganglionic transport of horseradish peroxidase. *J Comp Neurol* **216**, 162–174.

Labrakakis C, Lorenzo LE, Bories C, Ribeiro-da-Silva A & De Koninck Y (2009). Inhibitory coupling between inhibitory interneurons in the spinal cord dorsal horn. *Mol Pain* **5**, 24.

Lawson S (2005). The peripheral sensory nervous system: dorsal root ganglion neurons. In *Peripheral Neuropathy*, ed. Dyck P & Thomas P, pp. 163–202. WB Saunders; Elsevier, Inc.

Leong D, Puil E & Schwarz D (2004). Ketamine blocks non-N-methyl-D-aspartate receptor channels attenuating glutamatergic transmission in the auditory cortex. *Acta Otolaryngol* **124**, 454–458.

Li J & Baccei ML (2009). Excitatory synapses in the rat superficial dorsal horn are strengthened following peripheral inflammation during early postnatal development. *Pain* **143**, 56–64.

Liu Y, Broman J & Edvinsson L (2008). Central projections of the sensory innervation of the rat middle meningeal artery. *Brain Res* **1208**, 103–110.

Lu J, Zhou XF & Rush RA (2001). Small primary sensory neurons innervating epidermis and viscera display differential phenotype in the adult rat. *Neurosci Res* **41**, 355–363.

Lu V, Moran T, Balasubramanyan S, Alier K, Dryden W, Colmers W & Smith P (2006). Substantia gelatinosa neurons in defined-medium organotypic slice culture are similar to those in acute slices from young adult rats. *Pain* **121**, 261–275.

Lu Y & Perl ER (2003). A specific inhibitory pathway between substantia gelatinosa neurons receiving direct C-fiber input. *J Neurosci* **23**, 8752–8758.

McMahon SB, Armanini MP, Ling LH & Phillips HS (1994). Expression and coexpression of Trk receptors in subpopulations of adult primary sensory neurons projecting to identified peripheral targets. *Neuron* **12**, 1161–1171.

Melnick IV (2011). A-type K^+ current dominates somatic excitability of delayed firing neurons in rat substantia gelatinosa. *Synapse* **65**, 601–607.

Melnick IV, Santos SF, Szokol K, Szucs P & Safronov BV (2004). Ionic basis of tonic firing in spinal substantia gelatinosa neurons of rat. *J Neurophysiol* **91**, 646–655.

Mirnics K & Koerber HR (1995). Prenatal development of rat primary afferent fibers: II. Central projections. *J Comp Neurol* **355**, 601–614.

Morch CD, Hu JW, Arendt-Nielsen L & Sessle BJ (2007). Convergence of cutaneous, musculoskeletal, dural and visceral afferents onto nociceptive neurons in the first cervical dorsal horn. *Eur J Neurosci* **26**, 142–154.

Narayanan CH, Fox MW & Hamburger V (1971). Prenatal development of spontaneous and evoked activity in the rat (*Rattus norvegicus albinus*). *Behaviour* **40**, 100–134.

Neuhuber WL, Sandoz PA & Fryscak T (1986). The central projections of primary afferent neurons of greater splanchnic and intercostal nerves in the rat. A horseradish peroxidase study. *Anat Embryol (Berl)* **174**, 123–144.

O'Rahilly R & Muller F (2002). The two sites of fusion of the neural folds and the two neuropores in the human embryo. *Teratology* **65**, 162–170.

Olesen J, Burstein R, Ashina M & Tfelt-Hansen P (2009). Origin of pain in migraine: evidence for peripheral sensitisation. *Lancet Neurol* **8**, 679–690.

Panfil C, Makowska A & Ellrich J (2006). Brainstem and cervical spinal cord Fos immunoreactivity evoked by nerve growth factor injection into neck muscles in mice. *Cephalalgia* **26**, 128–135.

Perry MJ & Lawson SN (1998). Differences in expression of oligosaccharides, neuropeptides, carbonic anhydrase and neurofilament in rat primary afferent neurons retrogradely labelled via skin, muscle or visceral nerves. *Neuroscience* **85**, 293–310.

Prescott SA & De Koninck Y (2002). Four cell types with distinctive membrane properties and morphologies in lamina I of the spinal dorsal horn of the adult rat. *J Physiol* **539**, 817–836.

Qin C, Chen JD, Zhang J & Foreman RD (2007). Characterization of T9-T10 spinal neurons with duodenal input and modulation by gastric electrical stimulation in rats. *Brain Res* **1152**, 75–86.

Ruda MA, Ling QD, Hohmann AG, Peng YB & Tachibana T (2000). Altered nociceptive neuronal circuits after neonatal peripheral inflammation. *Science* **289**, 628–631.

Ruscheweyh R & Sandkuhler J (2002). Lamina-specific membrane and discharge properties of rat spinal dorsal horn neurones in vitro. *J Physiol* **541**, 231–244.

Safronov BV (1999). Spatial distribution of Na^+ and K^+ channels in spinal dorsal horn neurones: role of the soma, axon and dendrites in spike generation. *Prog Neurobiol* **59**, 217–241.

Schnoebel R, Wolff M, Peters SC, Brau ME, Scholz A, Hempelmann G, Olschewski H, Olschewski A (2005). Ketamine impairs excitability in superficial dorsal horn neurones by blocking sodium and voltage-gated potassium currents. *Br J Pharmacol* **146**, 826–833.

Spencer SJ, Hyland NP, Sharkey KA & Pittman QJ (2007). Neonatal immune challenge exacerbates experimental colitis in adult rats: potential role for TNF-α. *Am J Physiol Regul Integr Comp Physiol* **292**, R308–315.

Sterling M, Kenardy J, Jull G & Vicenzino B (2003). The development of psychological changes following whiplash injury. *Pain* **106**, 481–489.

Strassman AM, Mineta Y & Vos BP (1994). Distribution of fos-like immunoreactivity in the medullary and upper cervical dorsal horn produced by stimulation of dural blood vessels in the rat. *J Neurosci* **14**, 3725–3735.

Sugiura Y, Lee CL & Perl ER (1986). Central projections of identified, unmyelinated (C) afferent fibres innervating mammalian skin. *Science* **234**, 358–361.

Sugiura Y, Terui N & Hosoya Y (1989). Difference in distribution of central terminals between visceral and somatic unmyelinated (C) primary afferent fibers. *J Neurophysiol* **62**, 834–840.

Todd AJ (2010). Neuronal circuitry for pain processing in the dorsal horn. *Nat Rev Neurosci* **11**, 823–836.

Turrigiano G, Abbott LF & Marder E (1994). Activity-dependent changes in the intrinsic properties of cultured neurons. *Science* **264**, 974–977.

Vuillerme N & Pinsault N (2009). Experimental neck muscle pain impairs standing balance in humans. *Exp Brain Res* **192**, 723–729.

Walsh MA, Graham BA, Brichta AM & Callister RJ (2009). Evidence for a critical period in the development of excitability and potassium currents in mouse lumbar superficial dorsal horn neurons. *J Neurophysiol* **101**, 1800–1812.

Watson C, Paxinos G & Kayalioglu G (2009). *The Spinal Cord*. Academic Press, London.

Willis WD Jr (2007). The somatosensory system, with emphasis on structures important for pain. *Brain Res Rev* **55**, 297–313.

Willis WD & Coggeshall RE (2004). *Sensory Mechanisms of the Spinal Cord*, vol. 1. p. 271, Kluwer, New York.

Woodbury CJ, Ritter AM & Koerber HR (2000). On the problem of lamination in the superficial dorsal horn of mammals: a reappraisal of the substantia gelatinosa in postnatal life. *J Comp Neurol* **417**, 88–102.

Xu G-Y, Winston JH, Shenoy M, Yin H & Pasricha PJ (2006). Enhanced excitability and suppression of A-type K^+ current of pancreas-specific afferent neurons in a rat model of chronic pancreatitis. *Am J Physiol Gastrointest Liver Physiol* **291**, G424–431.

Yasaka T, Tiong SY, Hughes DI, Riddell JS & Todd AJ (2010). Populations of inhibitory and excitatory interneurons in lamina II of the adult rat spinal dorsal horn revealed by a combined electrophysiological and anatomical approach. *Pain* **151**, 475–488.

Yoshimura M & Jessell TM (1989*a*). Membrane properties of rat substantia gelatinosa neurons in vitro. *J Neurophysiol* **62**, 109–118.

Yoshimura M & Jessell TM (1989*b*). Primary afferent-evoked synaptic responses and slow potential generation in rat substantia gelatinosa neurons in vitro. *J Neurophysiol* **62**, 96–108.

Yoshimura N & de Groat WC (1999). Increased excitability of afferent neurons innervating rat urinary bladder after chronic bladder inflammation. *J Neurosci* **19**, 4644–4653.

Zeilhofer HU (2005). Synaptic modulation in pain pathways. *Rev Physiol Biochem Pharmacol* **154**, 73–100.

Zhou Q, Imbe H, Dubner R & Ren K (1999). Persistent Fos protein expression after orofacial deep or cutaneous tissue inflammation in rats: implications for persistent orofacial pain. *J Comp Neurol* **412**, 276–291.

Author contributions

All experiments were conducted in the School of Biomedical Sciences & Pharmacy at the University of Newcastle. M.A.T., A.M.B., B.A.G. and R.J.C. conceived and designed the experiments. M.A.T., B.M.H. and W.B.A. collected, analysed and interpreted the data. M.A.T., A.M.B., B.A.G. and R.J.C. drafted the article.

Acknowledgements

This work was supported by the National Health and Medical Research Council of Australia (Grants 401244, 569206, 628765), the Hunter Medical Research Institute, and the University of Newcastle, Australia.